2022/23 Status Report of China Nuclear Data Center

Shu Nengchuan, Wang Jimin, Huang Xiaolong, Xu Ruirui, Liu Lile, Tian Yuan, Sun Xiaodong, Zhangyue, Tao Xi

China Nuclear Data Center (CNDC)
China Committee of Nuclear Data
(CCND) China Institute of Atomic Energy
(CIAE)
P.O.Box 275-41, Beijing 102413, P.R.China, E-mail: gezg@ciae.ac.cn

General Information of China Nuclear Data Center

China Nuclear Data Center (CNDC) was established in 1975 and has been participating in the International Atomic Energy Agency's nuclear data activities as the National Nuclear Data Center of China since 1984. As a window, CNDC has been open to the world since 1978 and has established good cooperative relationships with the International Atomic Energy Agency, OECD/National Energy Agency, as well as major nuclear data centers and institutions around the world.

1.1 The current main task of CNDC

1) Management of domestic nuclear data activities.
2) Nuclear data evaluations, libraries and relevant methodology studies.
3) Nuclear data measurements and methodology studies
4) Exchange of nuclear data activities with IAEA, foreign nuclear data centers and agencies.
5) Services for domestic and foreign nuclear data application users.

1.2 Mainly Tasks of CNDC in 2022/2023

1) Five-Year-Plan (2021-2025) for nuclear data (CENDL Project).
2) Data evaluation for next CENDL version and sub-library.
3) Methodology studies of nuclear data evaluation (incl. theoretical and experimental for fission process…).
4) Nuclear data measurements and related methodology studies.
5) Compilations for EXFOR.
6) Nuclear data services.

Nuclear Data Evaluation

2.1 Neutron Activation File – CNAF

The first release CENDL-CNAF included 818 nuclei from ^{1}H to ^{257}Fm within the neutron energy region of from 10^{-5} eV to 20 MeV. The ENDF/B-6 data format was adopted. The general information, comments (MF=1), reactions cross sections (MF=3), nucleus dictionary (MF=8), and split threshold reaction channels (MF=10) are included in the library. Evaluations were obtained using APMN, Unified Hauser-Feshbach and Exciton model (UNF series), Full and Diagonal Reduced R-matrix (FDRR) model calculations or systematic analysis based on available experimental data. When there have many experimental data for a reaction channel, the evaluated experimental data were selected for curve fitting by using a program of orthogonal polynomial fit or spline function fit from threshold to 20 MeV. The fitting results were adopted. For convenient used in applications, all resonance parameters are already converted into a linearized point-wise format, and reasonably connected at the boundary

energy. To calculate the point-wise cross, The ENDF/B Pre-processing codes (PREPRO) were used.

2.2 Radioactive Decay Data File: CENDL-3.2/DDL

The CENDL-3.2/DDL included 2350 nuclei between A=66 to A=172 FY region. ENSDF and ENDF format were adopted. Evaluations taken from: (1) CNDC+ Jilin Univ.: ~500 nuclei; (2) DDEP: ~200 nuclei; (3) ENSDF: ~1500 nuclei; (4) JEF3.2: ~150 nuclei (only for stable nuclei). The Q-values of the decay modes are updated to the Atomic Mass Evaluation (AME) released in 2021Wa16. Jπ for g.s. (Jilin Univ.): by systematical comparison, physical analysis and theoretical calculation, spin for ground states is re-assigned for which lacks measurement or questionable. All T1/2 are revised by new measurements (2021, 12). Mean energies for β & γ: from TAGS measurements when available, otherwise from theoretical calculation. For even-even nuclides, from theoretically analysis which employed the self-consistent quasi-particle random phase approximation (QRPA) approach based on covariant density functional theory (CDFT) in Jilin University. Beta-delayed n, p, α emitted are adopted: P1n, P2n from eva. of 2015Bi05, 2020Li32; P1p,P1α from eva. of 2020Ba07 when measurements available, otherwise from systematics or theoretical calculation.

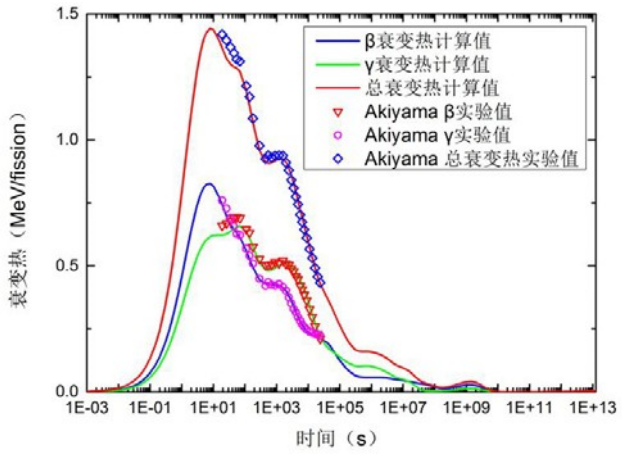

Fig. 1 Decay heat after ^{235}U fast neutron fission.

2.3 CENDL Photonuclear Data file: CENDL-3.2/PD

The photonuclear data (PD) for a total number of 264 materials are all newly evaluated and outputted with the standard ENDF-6 format. All of the photonuclear data are mainly evaluated based on the theoretical calculations with the Chinese photonuclear reaction codes GLUNF for the 6 light nuclei and MEND-G for the 264 medium-heavy nuclei. The incident photon energies for the medium-heavy nuclei are up to 200MeV. In order to extend the incident energy to 200MeV, the n, p, d, t, He-3, α are considered to totally 18th particle emission reactions in the MEND-G code.

To ensure the availability and reliability of the PD file, nuclear data processing code system NJOY2016 and MCNP6 are used to verify and validate the PD library. The testing results show that the data structure of each nuclide is complete, the data content is reasonable, and can be applied to the simulation of Monte Carlo transport.

Table 1 Nuclides List of CENDL-3.2/PD

Type	Nuclides	Count
Light elements	Be-9,B-10,11,C-12,N-14,O-16	6
Medium-heavy elements	Mg-25,26,Al-27,Si-28,29,30,P-31,S-32,33,34,36,Cl-35,37,Ar-36,38,40,K-39,40,41, Ca-40,42,43,44,46,Sc-45,Ti-46,47,48,49,50,V-50,51,Cr-50,52,53,54,Mn-55, Fe-54,56,57,58,Co-59,Ni-58,60,61,62,64,Cu-63,65,Zn-64,66,67,68,70,Ga-69,71, Ge-70,72,73,74,76,As-75,Se-74,76,77,78,80,82,Br-79,81,Kr-78,80,82,83,84,86,Rb-85,87, Sr-84,86,87,88,Y-89,Zr-90,91,92,94,96,Nb-93,Mo-100,92,94,95,96,97,98, Ru-100,101,102,104,96,98,99,Rh-103,Pd-102,104,105,106,108,110,Ag-107,109, Cd-106,108,110,111,112,113,114,116,In-113,115, Sn-112,114,115,116,117,118,119,120,122,124,Sb-121,123, Te-120,122,123,125,126,128,130,I-127,Xe-124,126,128,129,130,131,132,134,136,Cs-133, Ba-130,132,134,135,136,137,138,La-138,139,Ce-136,138,140,142,Pr-141, Nd-142,143,144,145,146,148,150,Sm-144,147,148,149,150,152,154,Eu-151,153, Gd-152,154,155,156,157,158,160,Tb-159,Dy-156,158,160,161,162,163,164,Ho-165, Er-162,164,166,167,168,170,Tm-169,Yb-168,170,171,172,173,174,176,Lu-175,176, Hf-174,176,177,178,179,180,Ta-180,181,W-180,182,183,184,186,Re-185,187, Os-184,186,187,188,189,190,Ir-191,193,Pt-190,192,194,195,196,198,Au-197, Hg-196,198,199,200,201,202,204,Tl-203,205,Pb-204,206,207,208, Bi-209	258

Fundamental theory study for fission data

3.1 Dynamical process of nuclear fission

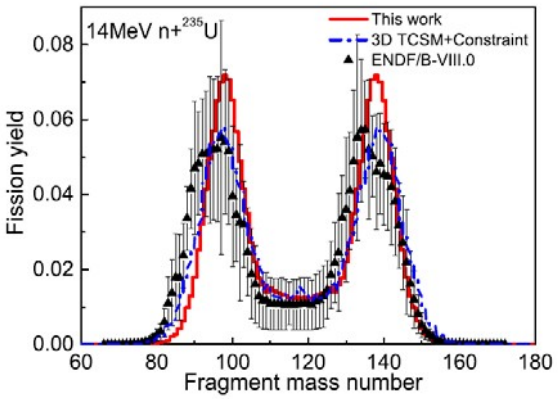

Fig. 2 Calculated fragment mass distribution of 14 MeV n + ^{235}U fission with the present model (red curve) compared with the result with the 3D Langevin approach plus a constraint on the heavy fragment deformation based on the TCSM (blue dashed-dot curve) and the evaluated data from ENDF/B-VIII.0.

The Langevin approach is extendedly applied to study the dynamical process of nuclear fission within the Fourier shape parameterization, with macroscopic energy – Lublin-Strasbourg Drop model, single-particle levels – Yukawa-folded potential, shell correction – Strutinsky method, pairing correction – BCS method. The results are shown in Figues

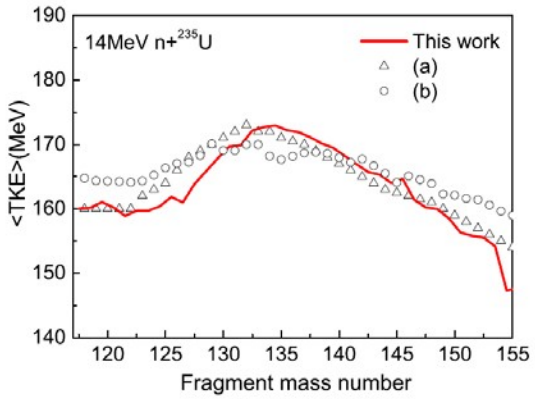

Fig. 3 The calculated TKE as a function of the heavy fragment mass in 14 MeV n + 235U fission compared with the experimental data.

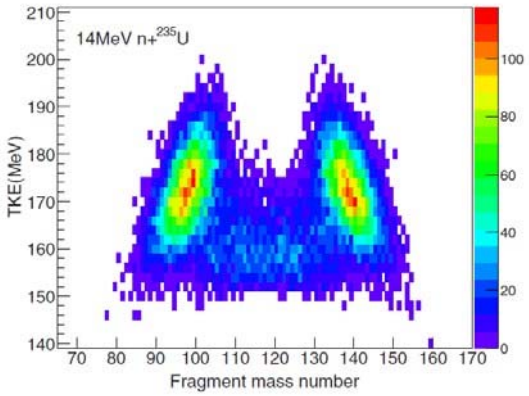

Fig. 4 The calculated mass-energy correlation of the fission fragments in 14 MeV n + ^{235}U fission.

3.2 Fission fragment mass distributions calculation

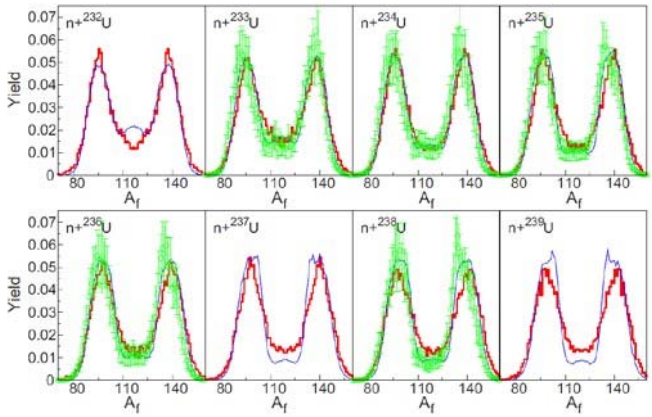

Fig. 5 The calculated fragment mass distribution in 14 MeV n +$^{232-239}$U fission (red curve), compared with the primary fragment mass distribution calculated with the GEF model (blue curve) and the evaluated data from ENDF/B-VIII.0 (green circle).

Using the 3D Langevin approach within the two-center shell model parameterization, the fission fragment mass distributions from 14 MeV neutron induced fission of U, Np and Pu isotopes , as well as the systematic dependence of the averaged TKE on the Coulomb parameter, are well reproduced.

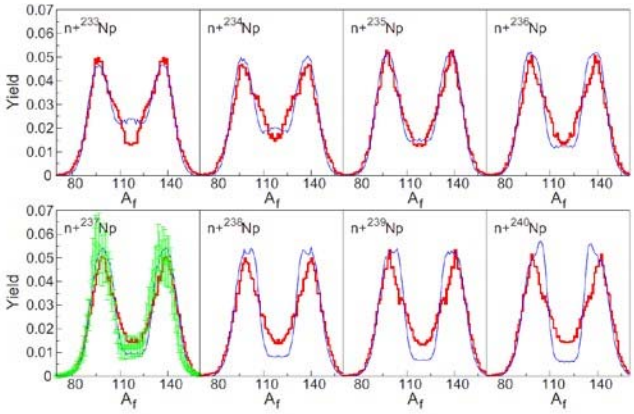

Fig.6 *The calculated fragment mass distribution of 14 MeV n + $^{233-240}$Np fission (red curve), compared with the primary fragment mass distribution calculated with the GEF model (blue curve) and the evaluated data from ENDF/B-VIII.0 (green circle).*

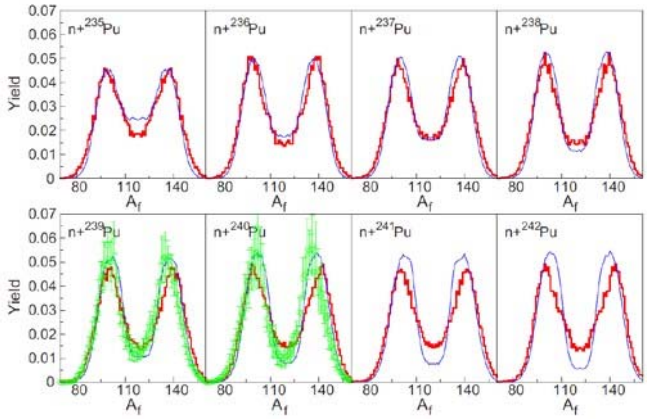

Fig. 6 The calculated fragment mass distribution of 14 MeV n + $^{235-242}$Pu fission (red curve), compared with the primary fragment mass distribution calculated with the GEF model (blue curve) and the evaluated data from ENDF/B-VIII.0 (green circle).

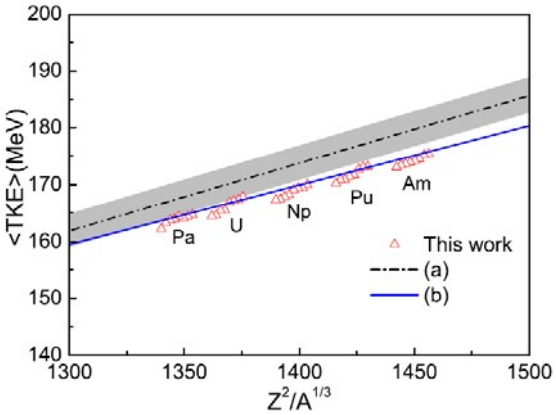

Fig. 7 The calculated systematic dependence of the averaged TKE on the Coulomb parameter Z2/A1/3 of the fissioning systems.

The influence of the neck parameter ε on the fission dynamics at low excitation energy is studied based on the three-dimensional Langevin approach in which the nuclear shape is described with the two-center shell model (TCSM) parameterization, and the elongation, the mass asymmetry and the fragment deformation are set to be the generalized coordinates of the Langevin equation.

Figure 9 shows the calculated fission fragment mass distributions using the Langevin approach with the ε taken to be 0.25, 0.35 and 0.45, respectively, and there is little difference between these results.

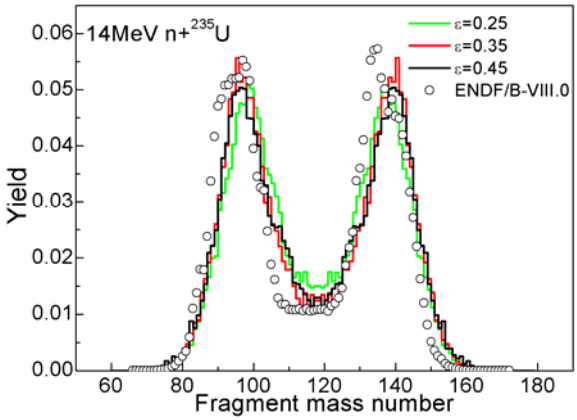

Fig. 8 The fragment mass distributions of 14 MeV n+^{235}U fission with the neck parameter ε fixed at 0.25, 0.35 and 0.45, respectively, compared with the evaluated data from ENDF/B-VIII.0.

Figure 10(a) shows the TKE distribution with the ε fixed at 0.25, 0.35 and 0.45, respectively, compared with the experimental data. One can see that the ε has a significant influence on the TKE calculation, which shows that with the increase of ε, the TKE increases and even the peak position of the TKE distribution is shifted toward the right side. The corresponding Coulomb repulsion energy at the scission point and the pre-scission kinetic energy are shown in Figs. 10(b) and 10(c), respectively. It can be seen that the overall behavior of the dependence of the Coulomb repulsion energy on the ε is similar to that of the dependence of the TKE distribution on the ε, and the ε has a very slight influence on the pre-scission kinetic energy, which indicates that the influence of the ε on the TKE mainly results from the Coulomb repulsion energy which is quite sensitive to the scission configuration. The slightly increase of the pre-scission kinetic energy with the ε decreasing may be due to the increase of the elongation of the fissioning nucleus around the scission point and simultaneously the decrease of Coulomb energy leading to a larger collective kinetic energy.

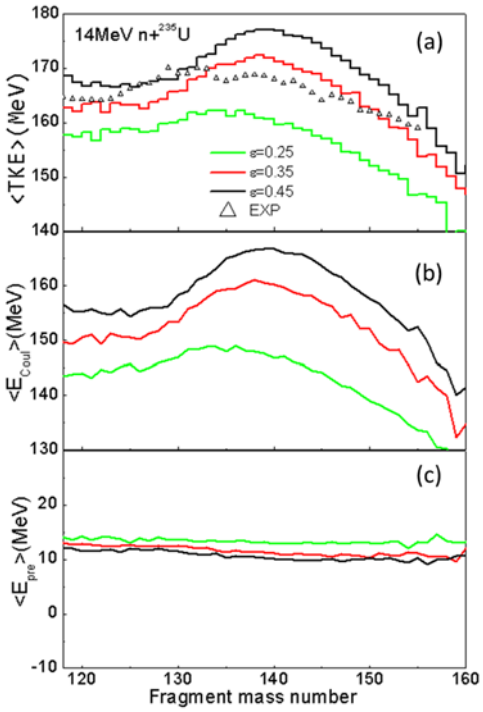

Fig. 9 The TKE distribution of fragments in 14 MeV n+^{235}U fission with the neck parameter ε fixed at 0.25, 0.35 and 0.45, respectively, together with the experimental data (a). The corresponding Coulomb repulsion energy at the scission point (b) and the pre-scission kinetic energy as a function of heavy fragment mass number (c) for different values of ε.

Progress of nuclear reaction theory

New version of the FUNF nuclear reaction program has been developed with a multiple fission barrier. Based on the earlier version of FUNF2012, we have added the multiple fission barriers model to the FUNF program. Now the FUNF program can calculate the fission cross-section with different kinds of fission barriers. For the case of the n+^{238}U reaction, the cross section calculated by the double fission barriers model is much better than the single fission barriers model, especially for the resonance structure in the low energy range, as shown in Fig.10.

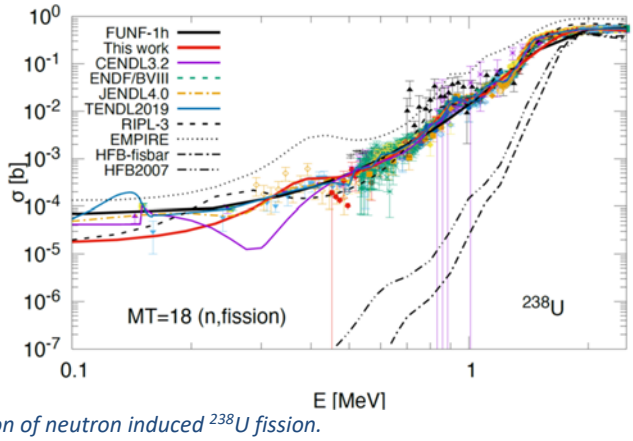

Fig. 10 Fission cross section of neutron induced ^{238}U fission.

The main excitation function on n+^{238}U reactions are evaluated at the energy region 0.1-20MeV, including (n, tot), (n, 2n), (n, f), (n, 3n), (n, γ) cross sections, and average number of fission neutrons NU. Partial evaluations are given in Fig. 11-Fig. 15.

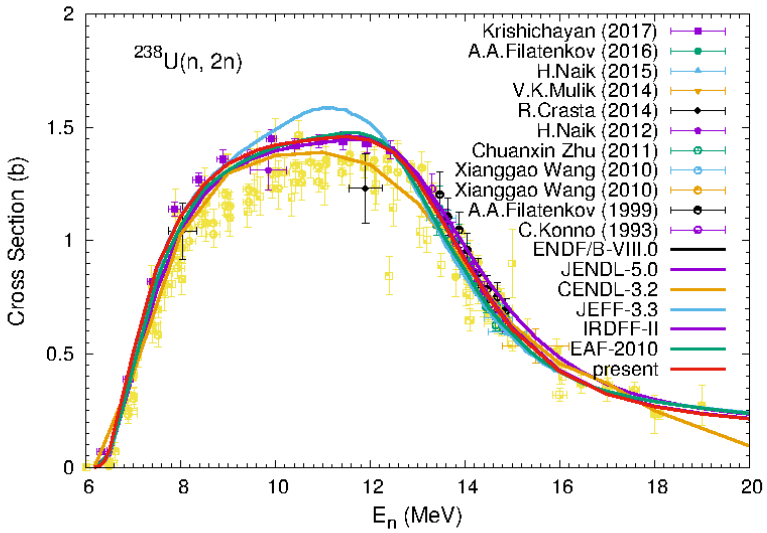

Fig. 11 Evaluated ^{238}U(n,2n) cross section

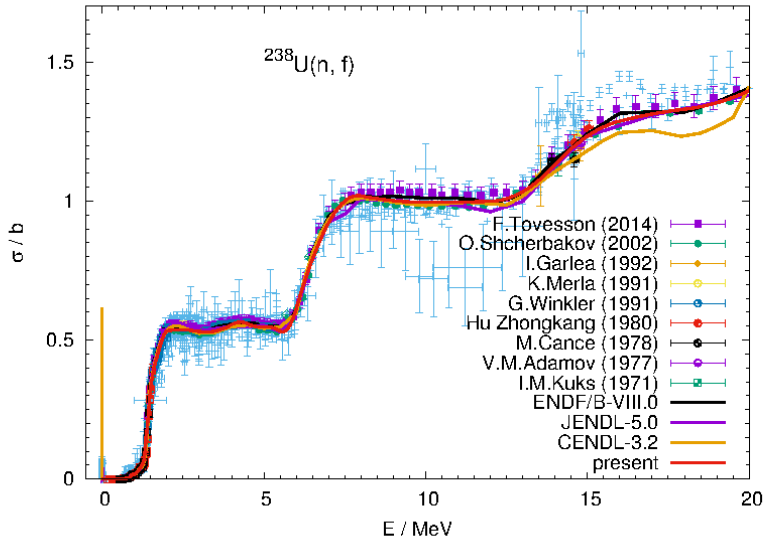

Fig. 12 Evaluated ^{238}U(n,f) cross section

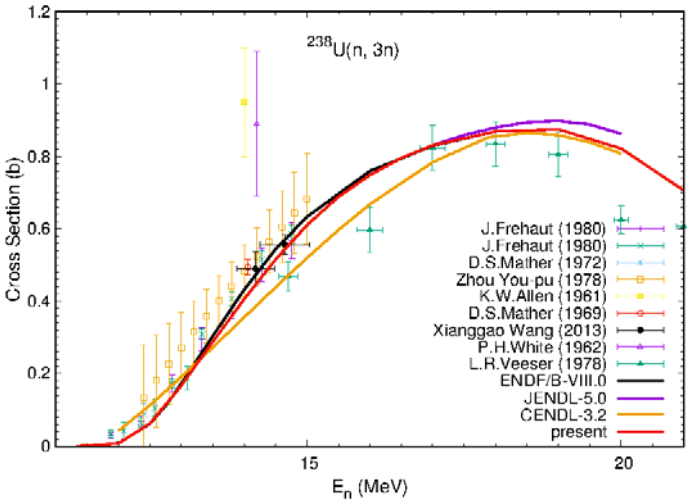

Fig. 13 Evaluated ^{238}U(n,3n) cross section

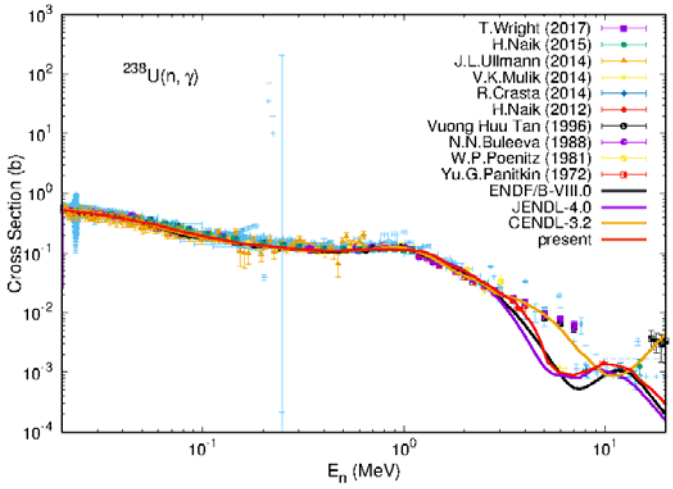

Fig. 14 Evaluated ^{238}U(n, γ) cross section

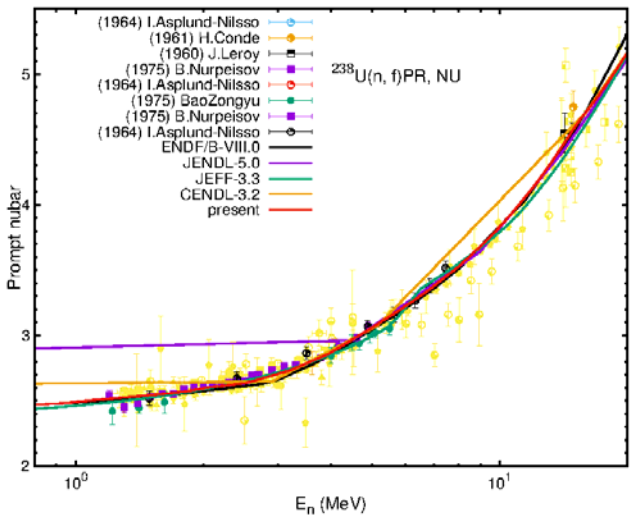

Fig. 15 Evaluated ^{238}U(n, γ) cross section

The whole set of nuclear data for n+^{238}U reactions, are calculated using nuclear theoretic model codes OPTMAN and FUNF at the neutron energy En≤ 20 MeV. Resonance parameters from ENDF/B-VIII.0 are adopted in the final data file. The integral benchmark calculations are also done for the n+^{238}U evaluated data. Fig. 16 shows the leakage flus spectra.

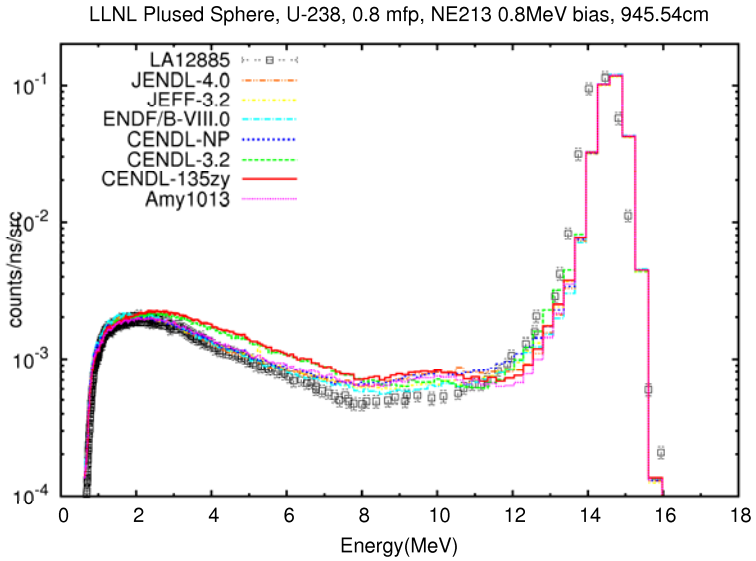

Fig. 16 calculated leakage flus spectra for n+^{238}U evaluations

EXFOR activities and nuclear data services

5.1 EXFOR Compilation

More than 475 entries were compiled at CNDC. Since 2010, more than 345 entries were finalized, which included 182 neutron and 163 charged particle entries. Feedback and correction were performed for more than 140 entries.

Since the last NRDC meeting (2022-06-01), 30 new entries have been finalized and 26 entries have been revised, more than 100 articles are under compiling, as shown in Fig. 17.

Currently CNDC is responsible for scanning of 8 journals published in China, namely ASI, CNPR, CNST, CPH/C, CPL, CST, HFH and NTC. The ASI is semimonthly, the HFH is bimonthly, the CNPR is quarterly and others are monthly. Scanning results are submitted to the IAEA/NDS monthly.

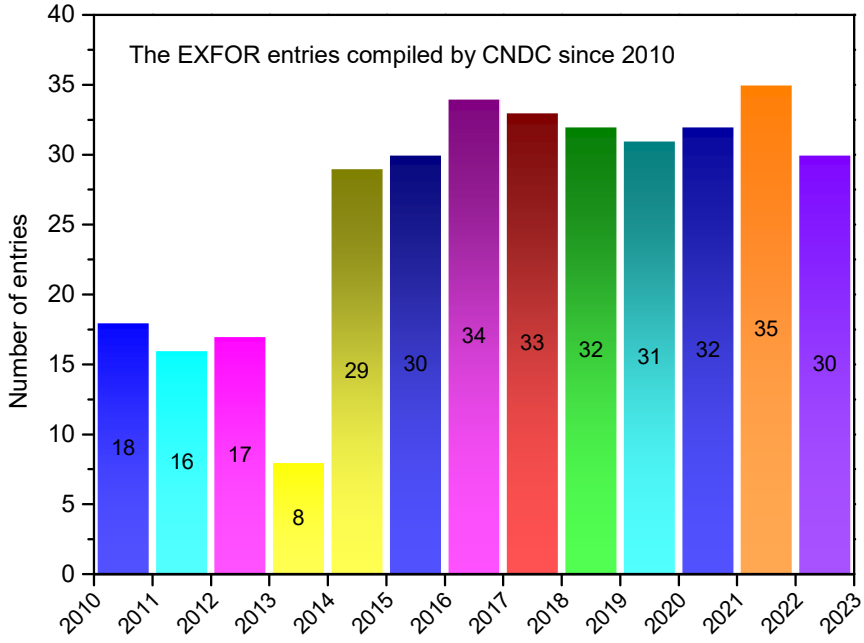

Fig. 17 The number of the finalized EXFOR entries

Table 2 New entries since the last NRDC meeting (2022-06-01)

No.	Entry No.	1st author	Reference	Status
1	32809	Luocheng Yang	J,ARI,164,109242,2020	Trans.3208
2	32810	X. X. Li	J,PR/C,106,065804,2022	Finalized
3	32811	Zhizhou Ren	J,PR/C,102,034604,2020	Trans.3208
4	32812	Junhua Luo	J,CPH/C,44,114002,2020	Trans.3208
5	32814	Yong Li	J,CPH/C,44,124001,2020	Finalized
6	32855	Junhua Luo	J,RCA,109,513,2021	Trans.3208
7	32856	Xin-Rong Hu	J,CNST,32,101,2021	Trans.3208
8	32857	S. Q. Yan	J,AJ,919,84,2021	Prelim.3209
9	32860	Luocheng Yang	J,ANE,165,108780,2022	Prelim.3209
10	32861	X. X. Li	J,PR/C,104,054302,2021	Finalized
11	32862	Zengqi Cui	J,EPJ/A,57,310,2021	Prelim.3209
12	32868	Zhang Jiang-Lin	J,ASI,71,052901,2022	Prelim.3209
13	32869	Wang De-Xin	J,ASI,71,072901,2022	Prelim.3209
14	32870	Jie Ren	J,CPH/C,46,044002,2022	Prelim.3209
15	32873	Yu.M.Gledenov	J,EPJ/A,58,86,2022	Prelim.3209
16	32886	Zhizhou Ren	J,EPJ/A,59,5,2023	Prelim.3209
17	32887	Yonghao Chen	J,PL/B,839,137832,2023	Finalized
18	32888	Chao Liu	J,NIM/A,1041,167319,2022	Finalized
19	S0087	Y.J.Li	J,PR/C,102,025804,2020	Trans.S031
20	S0235	F.F. Duan	J,PL/B,811,135942,2020	Trans.S031
21	S0249	Hua Wei	J,CNPR,34,138,2017	Trans.S031
22	S0261	Wang Tieshan	J,CST,35,496,2001	Trans.S031
23	S0262	Sun Xufang	J,CST,42,875,2008	Trans.S031
24	S0264	Su Xiaobin	J,CST,50,395,2016	Trans.S031
25	S0270	B.Liu	J,ARI,173,109713,2021	Trans.S031
26	S0273	W. H. Ma	J,PR/C,103,L061302,2021	Trans.S031
27	S0277	Y. Z. Sun	J,PR/C,104,014310,2021	Trans.S031
28	S0278	Hao Zhang	J,CPH/C,45,084108,2021	Trans.S032
29	S0279	Z. Y. Zhang	J,PRL,126,152502,2021	Trans.S032
30	S0295	B.Gao	J,PRL,129,132701,2022	Trans.S032

5.2 Nuclear data services and dissemination

CNDC provides the nuclear data service for institutes, universities or other requirements in China. The Fission Yield (1.0beta) App was developed by Jin Yongli at CNDC. This App can retrieve the fission product yield data of neutron-induced fission and spontaneous fission from various evaluated data libraries. The retrieved data can be shown as plot and saved in JPG and text formats for exchange.

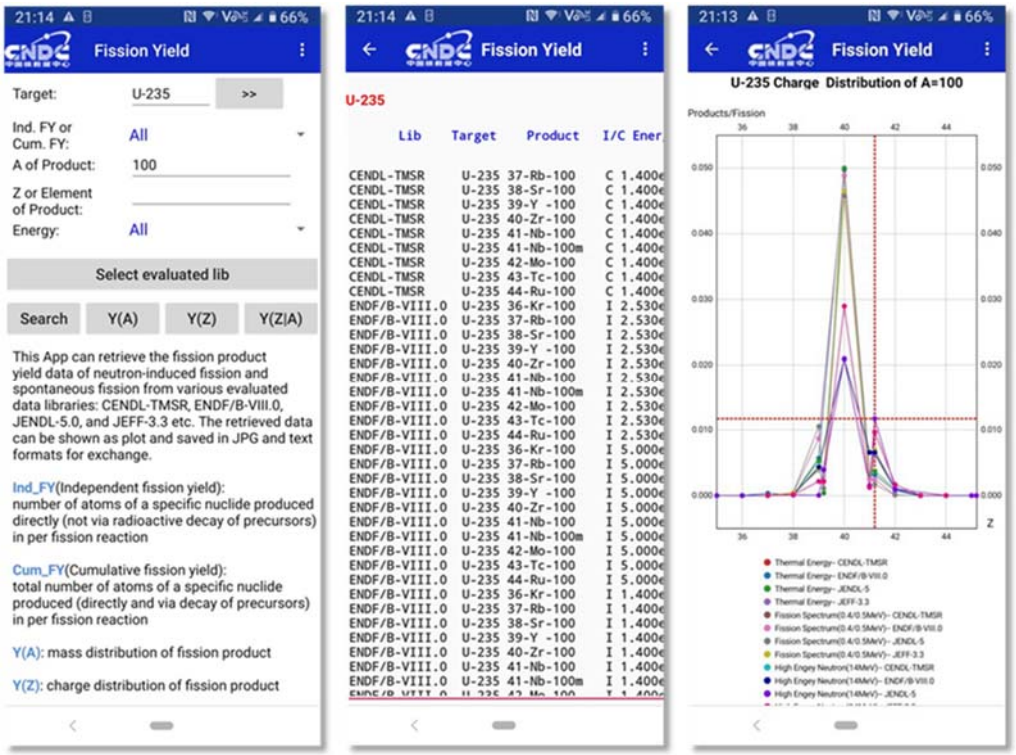

Fig. 18 Interface of the Fission Yield (1.0beta) App